13th ewtec 2019 Proceedings of the 13th European Wave and Tidal Energy Conference 1-6 Sept 2019, Naples, Italy

Simulation of Digital Displacement Hydraulic Power Take-Off for Wave Energy Converters

Sarah Acheson, Ross Henderson and Daniil Dumnov

***Abstract*—Designing a power take-off (PTO) for a wave energy converter (WEC) is a a serious technical challenge. Ideally a PTO would have smooth four-quadrant controllability, with high instantaneous power absorption across a broad range of incident wave periods and amplitudes, and efficient conversion to electricity. The Pelamis hydraulic PTO demonstrated many of these features, but the quantised nature of the applied PTO torque meant that the WEC response was not smooth and that instantaneous power absorption was reduced. Artemis Intelligent Power (AIP) have developed highly controllable and efficient hydraulic Digital Displacement®Pump Motors (DDPMs) which could be combined with the quantising features of the Pelamis PTO to give efficient, broad-band and smooth control. This concept is known as the Quantor PTO, and this paper presents the results of modelling the Quantor efficiency prior to testing. Across a range of four different input wave sets (including irregular seas) the simulated Quantor had an efficiency performance of between 64.7% and 70.9%. Primary conversion efficiencies were between 73.6% and 79.8%, and secondary conversion efficiencies were between 91 and 91.1%. Simulation results will subsequently be experimentally validated.**

***Index Terms*—Power take-off, hydraulic, wave energy**

I. Introduction

DESPITE the availability of a large potential global wave energy resource (estimated at 2.11 ± 0.05 TW [1]), wave energy conversion has not yet been deployed on a large commercial scale, although many different types and designs of WEC have been proposed [2]. This is due to the many technical challenges involved in converting energy from a random, reversing, high force, low speed resource with very high peak to mean power ratios to synchronous, grid quality electricity [3]. The subsystem of a WEC which performs this conversion from mechanical motion of the device to electricity is the PTO.

PTO design is a core challenge of realising the potential benefits of wave energy, as many of the technical difficulties of constructing a WEC culminate in this single subsystem. The desirable characteristics of a PTO include;

- Efficient instantaneous power absorption over a very broad range of wave amplitudes and periods
- Efficient conversion of variable instantaneous mechanical power to steady output electrical power
- Ability to efficiently handle power transferred at low speeds with high forces
- Responsive four-quadrant controllability of force and speed

This is not a full list of requirements as robustness to the marine environment, ease of assembly and maintenance, reliability and storm survivability and acceptable cost are also necessary to produce a commercially successful PTO [4], [5]. Hydraulic systems are a strong candidate for meeting these requirements, as they are inherently well-suited to applications with high forces and torques at low speeds. In contrast, electrical systems inherently struggle in this regime. They are also capable of providing energy storage in the form of gas pressure accumulators, which enables the smoothing out of peaks and troughs in the input power [3]. However the need for broad-band efficiency and precise four-quadrant controllability is not met by conventional hydraulics and novel approaches must be used to tackle these challenges. Conventional hydraulic transmissions can provide the variable load and flow required, but would need to be sized according to the maximum instantaneous power, which would mean that the average exported power would be in a very inefficient operating regime of the transmission [6]. For further detail on the challenges of WEC PTO design and the potential use of hydraulics, please see [7].

To maximise power extraction, an ideal PTO should be capable of control forces in a way which optimises the responses of the WEC in varying incident waves [8]. This generally means that the PTO should be able to both absorb and return energy to the WEC over the wave cycle to keep the system in resonance with the waves, so that the maximum power can be extracted and converted to electricity. Control of such reactive power flows was successfully demonstrated with full conversion efficiencies of 70% for a hydraulic PTO in Pelamis [9], but the 'quantised' PTO response meant that achieving continuous optimum PTO torque, as described in [8], was not possible.

Following the end of the Pelamis project, a proposal was put forward to combine the quantised PTO proven on Pelamis with a smaller continuously variable transmission of sufficient bandwidth to achieve the ideal continuous force control. The highly efficient, high bandwidth, hydraulic Digital Displacement pump motors (DDPMs) of AIP have the ability to act in combination with the quantised system to continually

This is paper ID 1283 submitted to the thematic track of grid integration, power and control. This work was supported in part by Wave Energy Scotland and by the EPSRC via the Industrial Doctoral Centre for Offshore Renewable Energy (IDCORE).

S. Acheson (an IDCORE student) and D. Dumnov work for Artemis Intelligent Power Ltd, Unit 3, Edgefield Industrial Estate, Loanhead EH20 9TB (e-mail: s.acheson@artemisip.com). R. Henderson works for Quoceant Ltd, Bonnington Bond, 2 Anderson Place, Edinburgh, EH6 5NP.

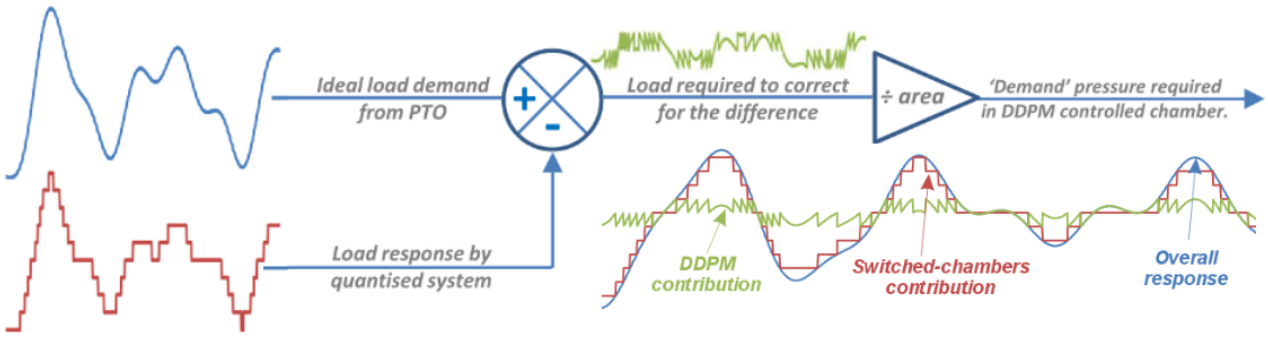

Fig. 1. Idealised Quantor concept taken from [4]. The error between the ideal load demand from the PTO (blue) and the load response from the quantised system (red) can be corrected using a DDPM capable of producing a rapidly changing load (green).

deliver the optimum continuous PTO force. (see [10] and [11] for an explanation of DD technology). This PTO concept is known as 'Quantor'.

Quoceant Ltd and AIP are working to develop and test the Quantor as part of a Wave Energy Scotland (WES) Stage 3 PTO project. A key deliverable of this project is the construction of a representative test rig, on which the Quantor can be experimentally tested. The test rig will have a 300kW motor which drives a flywheel with inertia of up to $973\,\mathrm{kg/m^2}$, which will provide a load representative of a WEC in irregular seas from which the Quantor will extract power. This project also involves building models of the Quantor, both for control strategy development and for efficiency modelling, the latter of which is presented here. For a discussion of the LCOE of Quantor, please see [4].

II. Description of Technology

The Quantor can be considered as an evolution of the Pelamis PTO. The Pelamis PTO used a novel digital approach to provide discrete set of net loads from pressurising or not pressurising individual piston areas. This 'quantised' system could approximate continuous control by choosing the number of discrete load steps which were enabled (pressurised) at any one time [6]. This system meant that absorbed power was transferred directly to (and from) the energy storage accumulators, so that instantaneous power absorption could be very high and absorbed power was decoupled from average exported power [12].

However, a disadvantage of this discretised system was that the PTO could only provide a quantised approximation to a continuously variable load, which did limit the power absorption [6] and made the system inapplicable to low inertia WEC types where the quantised resolution would have been too coarse. A compromise is required between the WEC mass, the quantised step size, and the resulting distortion in control. Control strategies which could yield power or reliability performance improvements rely on continuously variable PTO force to achieve optimal power capture.

Adding a continuously controlled load of the same range as one or more of the quantised load steps would make it possible to achieve continuous control across the full load and power range. For this to work, the control of the continuously variable load must be fast enough to compensate for the step changes in the underlying quantised load [6]. Fig.1 shows the idealised Quantor concept combining a quantised system with a continuously controlled load, producing a smooth PTO load which can follow the ideal demand from the controller.

Fig. 2 shows a simple schematic of the Quantor PTO with a single degree-of-freedom WEC with linear hydraulic actuators (cylinders). These cylinders have multiple chambers, like those used in Pelamis. As the WEC moves in heave, the Quantor PTO system must provide the required PTO load for extracting power, consisting of both resistive and reactive components. The quantised chambers are connected via the digitally controlled chamber switching valves (housed in manifold blocks) to either the accumulator or to tank. This means they provide steps of force or torque as shown by the red line in Fig. 1. Hydraulic energy collected by these quantised chambers from the WEC is buffered by the accumulator which functions as a compliant energy store. Meanwhile, the continuously controlled chamber is connected to DDPM B, which provides the smoothing contribution (green line in Fig. 1) by controlling the chamber pressure at high bandwidth. This rapidly varying pressure signal from DDPM B results in an irregular torque on the common fixed-speed shaft, which is connected to generator and the opposing DDPM machine (DDPM A). The role of DDPM A is both to counteract this irregular torque, smoothing the output to the generator shaft; and to extract energy from the accumulator to provide a net power export.

III. Description of Model

A. Model Overview

Whilst the Quantor PTO could function with either linear (multi-chambered cylinders as in Pelamis) or rotary (fixed displacement pump-motors) actuators, rotary actuators were chosen for the Quantor test rig, as they were more appropriate for the space available and more applicable to the current WEC market. Whilst Fig. 2 shows a WEC with a linear system as an example, the modelling work treated a rotary system as this will be available for validation on the test rig. Fig.3 shows

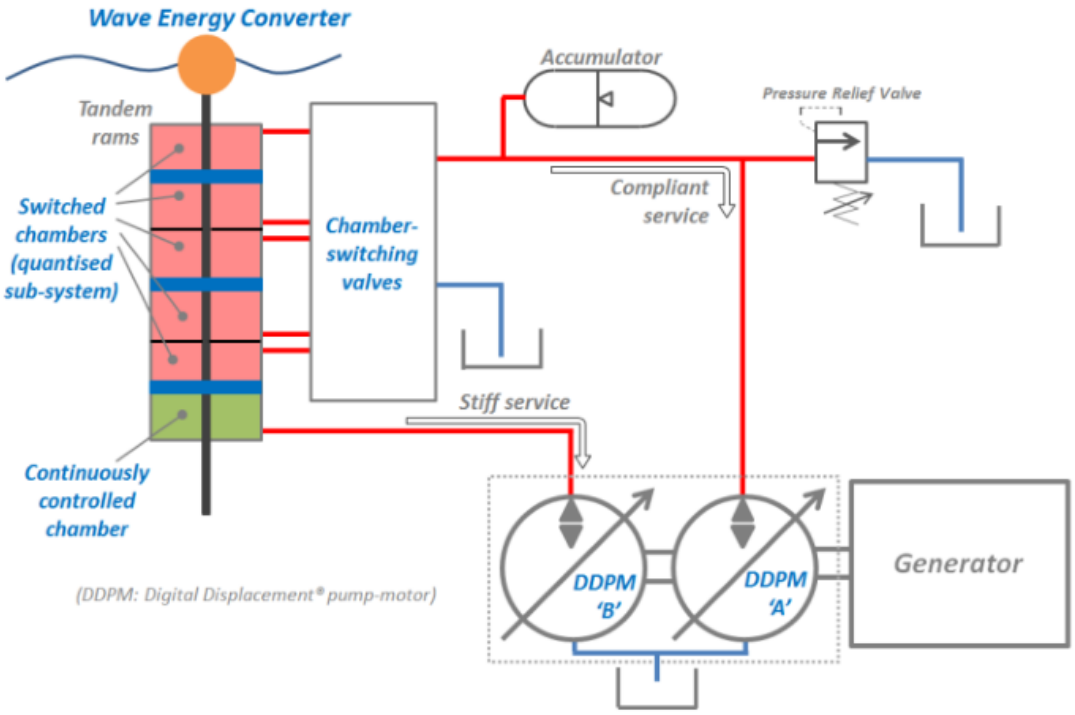

Fig. 2. Schematic of Quantor with linear actuator with single degree-of-freedom WEC. It should be noted that there is a manifold block containing switching valves connected to each chamber including the continuously controlled one, but it is omitted above to show the direct pressure control which DDPM B has over this chamber. [4]

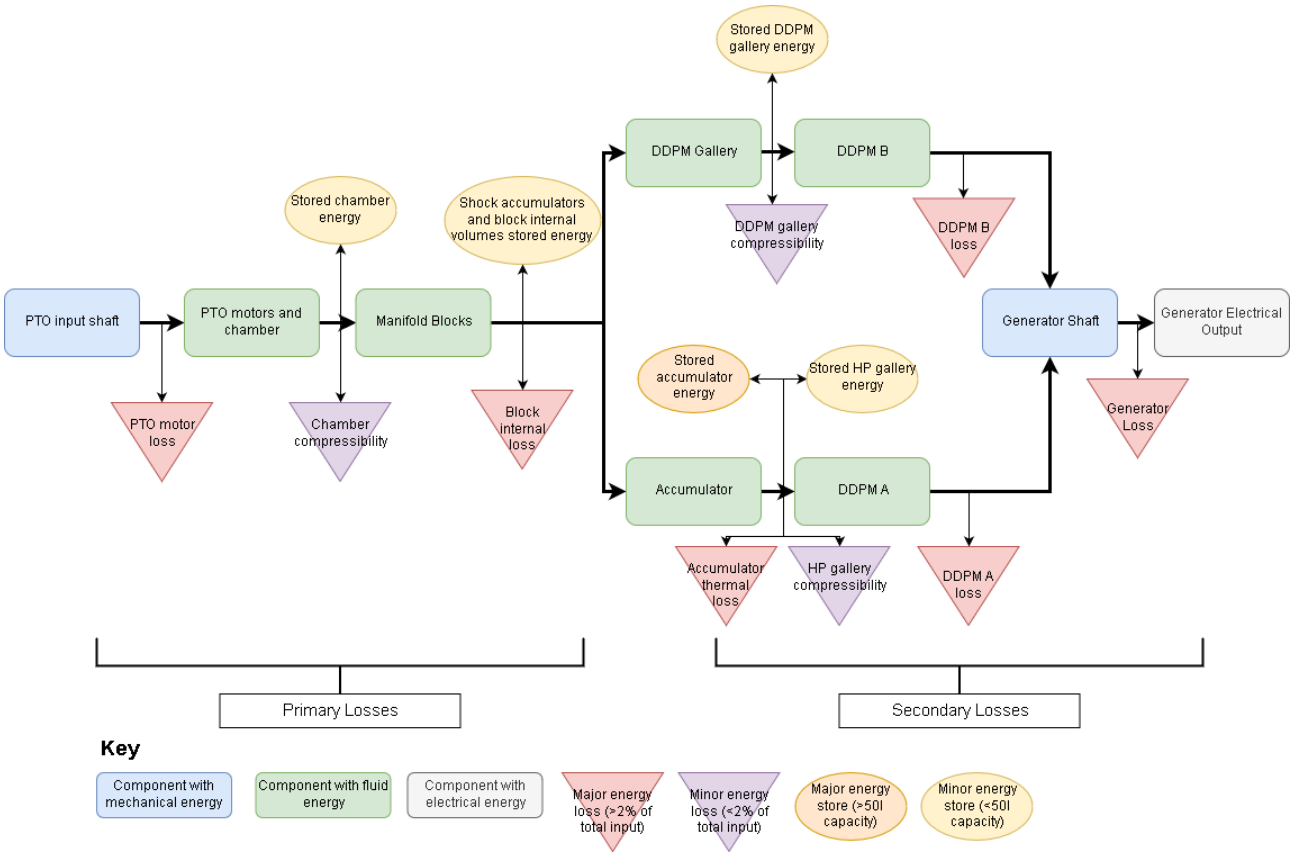

Fig. 3. Schematic of Quantor model structure, showing the flow of energy through key components, as well as the positions of energy stores and the energy losses measured at each stage in the model. The 'minor energy stores' are included in this figure because they are included in the model, but the energy stored in them is proportionally very small (0.4% or less) so it is assumed that any stored energy from these components is distributed pro rata to the remaining nodes.

an overview of the energy flow through the system, characterised by key components, energy stores and

measured losses in the model. The input to the system is the mechanical power on the PTO input shaft, which is mechanically driven by the relevant WEC system (in this case, by a winch and ring gear). Losses in the specific WEC systems prior to the PTO are not included in this model. This input PTO shaft connects to the multiple (in this example, four) PTO motors which, as they convert mechanical energy to fluid energy, will give rise to the first major losses of the system, due to leakage and friction as explained in III-G. Rotating machines introduce substantial additional losses over hydraulic cylinders but offer flexibility for different WEC designs (e.g. winches and hinges). The chamber refers to the volume of fluid via which the motors connect to the manifold blocks, the pressure of which dictates the applied load of the actuator. For rotating motors this volume is dominated by connecting pipework; in the equivalent linear system, this would be dominated by the volume of the chamber inside the cylinder. Volumetric losses can result from energy used to pressurise the oil in the chambers then being vented to tank as part of the control process. Energy is then transferred to the manifold blocks, where it can be lost internally via flow losses, valve pressure drops and valve leakages. Due to the shock accumulators mounted on the blocks' HP galleries and the internal fluid volumes of the block, some energy may be stored in the blocks or even extracted from the energy stores in the blocks, for example if the charge of the shock accumulators is lower at the end of the simulation than at the start. Depending on the control of the valves in the manifold blocks, the oil may then flow into the DDPM gallery (the 'stiff service') or into the accumulator (called the compliant service because the quantised chambers are connected to an accumulator). In both of these galleries, energy may be stored or lost to hose compliance. The system to be tested on the rig has a precharge pressure of 150bar with an oil volume of up to 74l and gas back-up bottles of a further 75l. This is scalable to much larger storage volumes in line with the PTO as a whole. The two DDPMs then convert the stored hydraulic energy back into mechanical energy applied to the generator shaft, on which they are both mounted. This conversion incurs energy losses to the system as well, which are defined by the loss model described in III-F. In converting the received mechanical energy to electrical energy the generator is not perfectly efficient as explained in III-H.

The losses are divided into primary and secondary losses according to the method proposed in [12], where the main HP accumulator divides the system. The primary losses are those incurred in delivering energy from the PTO input to the accumulator and the secondary losses are those incurred in delivering energy from the accumulator to the generator. However since there are two services, only one of which has an accumulator, this definition is less obvious than in the Pelamis system. Particularly this is because DDPM A is carrying the transforming function of counteracting the irregular torque output of DDPM B by exchanging energy with the accumulator, whilst simultaneously extracting energy from the accumulator to drive the generator. The transforming function can be considered a primary conversion process, whilst exporting to the generator is a secondary conversion process. It is not possible to distinguish the primary and secondary DDPM A losses using this model, so an equal split is assumed. Therefore the PTO motor losses, valve block losses, hydraulic hose losses, DDPM B losses and half of the DDPM A losses make up the primary losses, and the remaining half of the DDPM A losses, and the generator losses make up the secondary losses.

It should be noted that energy does not necessarily constantly flow in the directions shown; all the hydraulic machines involved can transfer power in either direction. However the arrows in Fig.3 represent the primary direction of energy flow for electricity generation. Total PTO efficiency is defined as the ratio of the electrical energy generated to total mechanical energy available to the PTO from the wave induced WEC motion. This PTO efficiency does not include hydrodynamic or other losses in the WECs primary absorption mechanism.

The hydraulic system is simulated using Simscape, which is a physical modelling package within the wider Matlab/Simulink environment. The AIP DDPM loss models are built in Simulink.

B. PTO Control Strategy

The PTO control strategy chosen was reactive control with a spring term, as described in [7] by 1 where τ_{PTO} is the demanded PTO torque, c_{PTO} is the damping coefficient, ω is the rotational speed of the PTO shaft, k_{PTO} is the spring coefficient and θ is the angular position of the PTO shaft. The addition of the spring term means that the frequency response of the WEC can be shifted towards resonance in non-resonant conditions, improving net power absorption. The Quantor tested in the laboratory will have a maximum PTO torque of 1.4kNm but this could be easily increased by adding more fixed displacement motors to the system.

$$\tau_{PTO} = c_{PTO}\omega + k_{PTO}\theta \tag{1}$$

C. Wave and WEC model

The model was used to simulate a WEC with a Quantor PTO in both regular and irregular waves, of two different scales each. For the regular waves the simulation was 300s long and for irregular seas the simulation was 512s long. The difference was because it was simply necessary to allow the regular simulation to reach a steady state, whereas for the irregular sea, 512s is a reasonable minimum length of time required for the WEC to experience a representative range of waves from the chosen sea spectrum. The irregular waves were modelled using a JONSWAP spectrum with a gamma factor of 1 and timeseries were produced using the WAFO Matlab toolbox [13]. The details of each set of waves are given in Table III-C. The power per unit crest length (or wave energy flux per unit crest length in the case of irregular waves) is given by (2) for regular waves [14] and by (3) for irregular waves [15]. These were chosen such that there was both a

TABLE I
CHARACTERISTICS OF DIFFERENT INPUT WAVES USED FOR SIMULATION

Input Waves	T	T_p(s)	T_e (s)	H_s (m)	Wave power per unit crest length (kW/m)
Regular 1 (R1)	7.5			2.5	45.9
Regular 2 (R2)	8.5			3.5	102.1
Irregular 1 (I1)		7.7	6.6	2.5	20.2
Irregular 2 (I2)		9.1	7.8	3.5	46.9

low and high energy example of regular and irregular waves. R1 and I2 were very similar in terms of the wave energy density, and the four different wave sets together provide a broad spread of input power per unit crest length, from 20 to 100 kW/m.

$$P = \frac{\rho g^2}{32\pi} H_s^2 T \tag{2}$$

$$P = \frac{\rho g^2}{64\pi} H_s^2 T_e \tag{3}$$

The WEC was modelled using a one-dimensional linear hydrodynamic equation of motion. The WEC modelled was a simple heaving sphere of 4.5m diameter. The modelled architecture was a winch PTO system, attached to a ring gear, on the circumference of which the fixed displacement motors of the Quantor PTO are mounted. This means the fixed displacement motors on the test rig to run at the same speed as they would on the simulated WEC, grounding the hardware-in-the-loop system in the reality of a sea-based deployment.

D. Valve Block Model

The manifold block has many functions within the Quantor, but the main purpose is that it connects the appropriate motor ports to either the HP gallery, DDPM gallery or LP gallery according to the real-time control algorithm. Each fixed displacement motor has its own corresponding manifold block to control its port connections. Each manifold block contains approximately forty valves, twelve of which are solenoid-operated and seven of which have tunable settings, such as adjustable needle valves.

The control valves were modelled as Simscape two-way directional valves controlled by two-position valve actuators, characterised by maximum area and opening. This assumes that the valve passage area is linearly dependent on control member displacement [16]. The valve models in Simscape include important loss characteristics (pressure drop) and have a user-specified transit time to simulate their dynamic behaviour. Dynamic behaviour due to spring loading and spool characteristics are omitted to keep complexity and simulation time manageable, given the large number of valve components in this system. Experiments have been carried out on each valve type to characterise its performance in terms of opening time and pressurisation curves for the chambers connected to

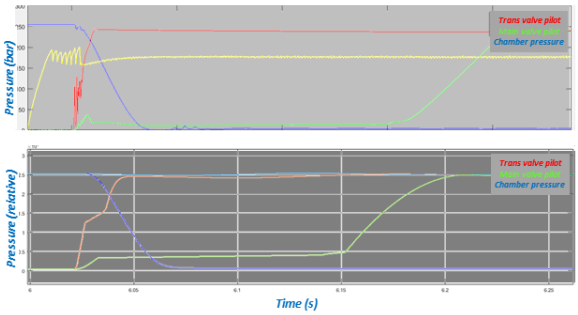

Fig. 4. Top: pressure data gathered showing two-stage depressurisation of a Quantor chamber, Bottom: model data of the same event after validation, with same time axis. The key comparisons are between the 'Trans valve pilot', 'Main valve pilot' and 'chamber pressure' curves.

that valve. These experiments were used to tune the model parameters and match the model to test data. Fig 4 gives an example comparison between valve test data and the model. This valve block model will be further refined with data from the full test rig.

E. Auxiliary Systems

The simulation of the hydraulic circuit includes all of the major hoses and piping connections between the hydraulic machines, manifold blocks and accumulators. The oil volumes within the galleries of the manifold blocks are also included, based on approximations derived from the manifold block design. The simulated hydraulic connections account for the bulk modulus of the oil volume in those connections (compliance), pressure drop due to the length and diameter of the connections, and in the case of hydraulic hoses, the additional compliance due to the expansion under pressure of the hose itself. Fluid inertia is omitted from this model since the purpose of this model is to study the performance and efficiency of the Quantor PTO, and the addition of fluid inertia to the hydraulic connections significantly increases the higher frequency dynamics of the system, and hence greatly slows down the simulation solution time without changing the overall system efficiency or performance. These higher order effects will of course be present on the test rig, and if they are significant then will need to be addressed. Since the hydraulic connections are fairly short it is not expected that inertial effects will present significant issues in practice. A single run in an irregular sea was carried out with and without fluid inertia and the results in terms of average power transferred at various key points in the model differed by a maximum of $0.02\,\mathrm{kW}$. Hydraulic accumulators are simulated using the standard polytropic gas model. A constant thermal efficiency value of 95% is used, assuming a foam-filled accumulator as described in [17].

The low pressure supply was modelled as Simscape Reservoir of volume $2\,\mathrm{m}^3$ with a constant pressure of 5 bar. On the test rig the low pressure may vary more due to changing volumes of oil as chambers are depressurised but the low pressure accumulator is so large ($75\,\mathrm{l}$ accumulator with $975\,\mathrm{l}$ of gas back-up bottles) that this effect should be minor.

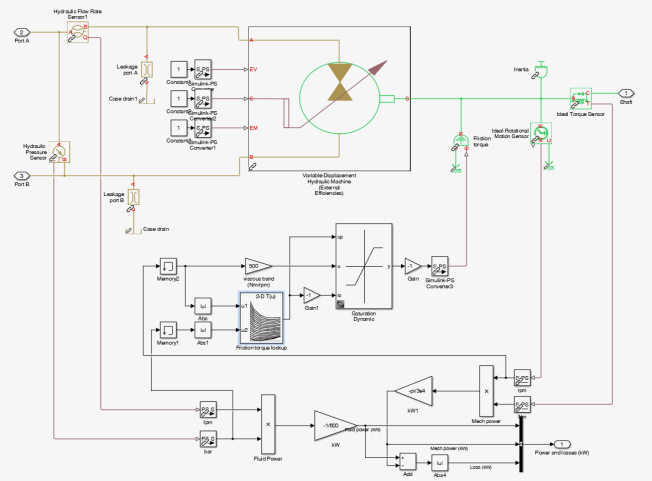

Fig. 5. Simulink and Simscape model of Poclain pump-motor, showing inclusion of leakage, friction torque and mechanical inertia.

F. DDPM Model

The DDPMs were modelled using existing Artemis Simulink models of their pumps, which are based on the loss model proposed by [10]. These are semi-empirical models based on test data collected from real machines at AIP. The loss models are based on data collected from machines operating as pumps, and it is assumed that the same losses apply for a machine acting as a motor. This is because all of the physical mechanisms of loss in the machine (leakage and friction) remain the same in motoring as in pumping and the duration of pressurisation of each cylinder in the machine is roughly the same in both cases. The model does account for the difference in effective displacement in pumping and motoring, since this is does have an impact on the overall ability to transmit power.

G. PTO Motor Model

The fixed displacement pump-motor selected for the test rig was a Poclain MS02 of $255\,\mathrm{cm}^3/\mathrm{rev}$. The manufacturer provided performance data which was used to model the friction torque and leakage, as shown in Fig. 5. It should be noted that any fixed displacement motor could be used in a rotary system. The system can be scaled up using much larger motors with similar efficiency characteristics. This particular model was chosen for its suitability to the rig-scale torques, speeds and flows, and for a real WEC of a different scale a different pump-motor may be more suitable.

The Simscape variable-displacement hydraulic machine block was chosen as this operates in both directions as a pump and a motor. However it was decided not to use its inbuilt 'external efficiencies' feature as efficiency curves often have very steep gradients at the corners of the map, causing problems with extrapolation and interpolation. Given we had measured data for output torque and leakage, it was a more direct approach to apply these to the shaft and the ports respectively. Hence the volumetric and mechanical efficiency of the motor were set to one, as was the displacement, as this is a fixed-displacement machine. For the leakage, a linear hydraulic resistance was used with a leakage corresponding to the manufacturer-supplied data. From the calculated friction torque, a lookup table was generated which was applied to the output shaft so that it reduced the output torque in both directions. The motor's internal inertia was also represented.

H. Generator

The electric generator on which the DDPMs are through-shafted was modelled very simply in Simulink, according to 4, where η is the provided motor manufacturer's estimated efficiency of 94.3%, ω is a constant generator speed of 1500rpm and τ is the total shaft torque, which is calculated by summing the torques of both DDPMs.

$$P = \eta\tau\omega \tag{4}$$

The reason this was simplified is that on the test rig to be used to validate the model, the measurement of output power will be the speed and torque on the generator shaft; not the electrical power generated. This is because the generator chosen for the test rig is not sized to the Quantor power regime but to give sufficient shaft diameter for the two DDPMs operating 'back-to-back' as a pump-motor test rig, making its electrical output unrepresentative of the intended WEC system. Also, an induction motor has been used here so that testing can be carried out at different speeds if required, whereas a real WEC deployment would more likely use a synchronous generator. There is little doubt over the established efficiency of standard electrical generators operating at fixed speed, so this does not undermine the model validation.

IV. Model Results

The modelled Quantor showed the ability to perform in all four quadrants of force and speed, and smooth overall output torque could be achieved with careful tuning of the control parameters. Fig. 6 shows a Sankey (energy flow) diagram of the results from modelling sea state I2. The results are shown in percentages of the total input energy on the PTO shaft. The nodes correspond to those shown in Fig. 3, but those where the percentage of the total energy reaching them is less than 0.1% are omitted for clarity. The accumulator starts and finishes the model run at the same pressure, so there is no net change in its stored energy. Any residual energy in the minor energy stores is assumed to be used 'pro-rata' by the following nodes.

The model result for total electrical energy output is 68.6% of the input energy, with 22.5% going to primary losses and 8.9% going to secondary losses.

From Fig. 6 it is clear that the greatest energy loss in the system is the PTO motors at 8.4%, followed closely by the primary control losses at 8.0%. These elements handle most of the power and therefore are expected to induce a substantial proportion of the losses. As previously mentioned, the PTO motors were chosen for the test rig and may not be the best choice for any given WEC, so this loss could be changed

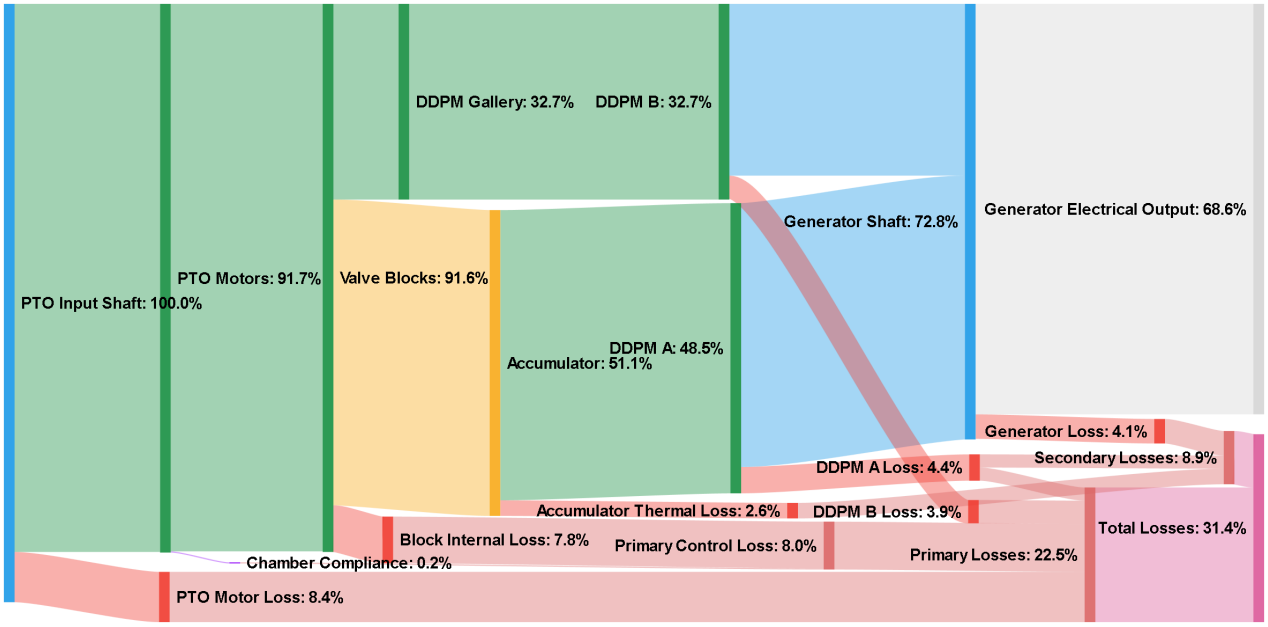

Fig. 6. Sankey diagram of model results of sea state I2, with energy flow going from left to right.

TABLE II
RESULTS OF MODELLING FOR DIFFERENT INPUT WAVES, IN TERMS OF AVERAGE INPUT POWER INCLUDING PRO-RATA ALLOCATION OF STORED ENERGY IN EFFICIENCY CALCULATION.

Input Waves	Average Model Input Power (kW)	Average Generated Power (kW)	Average Stored Power (kW)	Average Lost Power (kW)	Quantor Efficiency (%)
R1	40.3	28.4	0	11.9	70.5
R2	53.5	37.9	0.1	15.6	70.9
I1	25.9	16.8	0	9.2	64.7
I2	37.5	25.8	0.5	11.2	68.6

by selecting PTO motors of appropriate specification for the application. Larger motors for higher power applications also offer higher efficiency. The option of using linear actuators instead of motors would also greatly improve the efficiency of this step. The primary control losses comprise the loss caused by depressurising chambers and venting to tank, chamber compliance and losses within the valve block. The block internal losses could possibly be reduced by choosing different valves with lower pressure drops and by redesigning some of the internal galleries. Data from the test rig (e.g. pressure measurements along the flow paths) will allow refinement of the flow loss coefficients for the valves and their immediate flow paths.

The DDPM losses are the next most significant losses at 4.4% of the total on machine A and 3.9% on machine B. These are significantly impacted by the operating point of each machine in the chosen input waves. Depending on the operating point, DDPMs have shown efficiencies at 1500rpm (the chosen speed for the DDPMs on the test rig) ranging between 91% and 97% [10]. Generally the higher the displacement, the more efficiently the machine can operate. The average efficiency over this simulation run for DDPM A was 90.9% and for DDPM B was 87.9%. This is because the machines are operating at a lower average power than the optimum, particularly DDPM B. DDPM B has to operate at very low pressures and displacements due to the need for torque exerted by the stiff service to regularly pass through zero, which means the stiff service pressure must go as close to the LP system pressure as possible.

Table IV shows the key model results for all four wave sets in terms of absolute energy input, stored, generated and lost, as well as the percentage efficiency. This percentage energy assumes that the stored energy displayed in the table would be extracted through the generator 'pro-rata', were it to be used. Despite the large variation in the power density of the input waves (between 20 and 100 kW/m), the Quantor efficiency varies by only approximately 6%, with 64.7% being the minimum and 70.9% being the maximum.

The results for R1 and R2 are very similar in terms of efficiency and loss breakdown (see Fig. 7). This is because both wave sets are using the full range of the Quantor system, and in R2, which is the higher energy wave set, the PTO load is fully saturated at the peak where the PTO motors cannot exert any more torque. It is encouraging to note that once the full load range of the Quantor is exercised, saturation did not lead

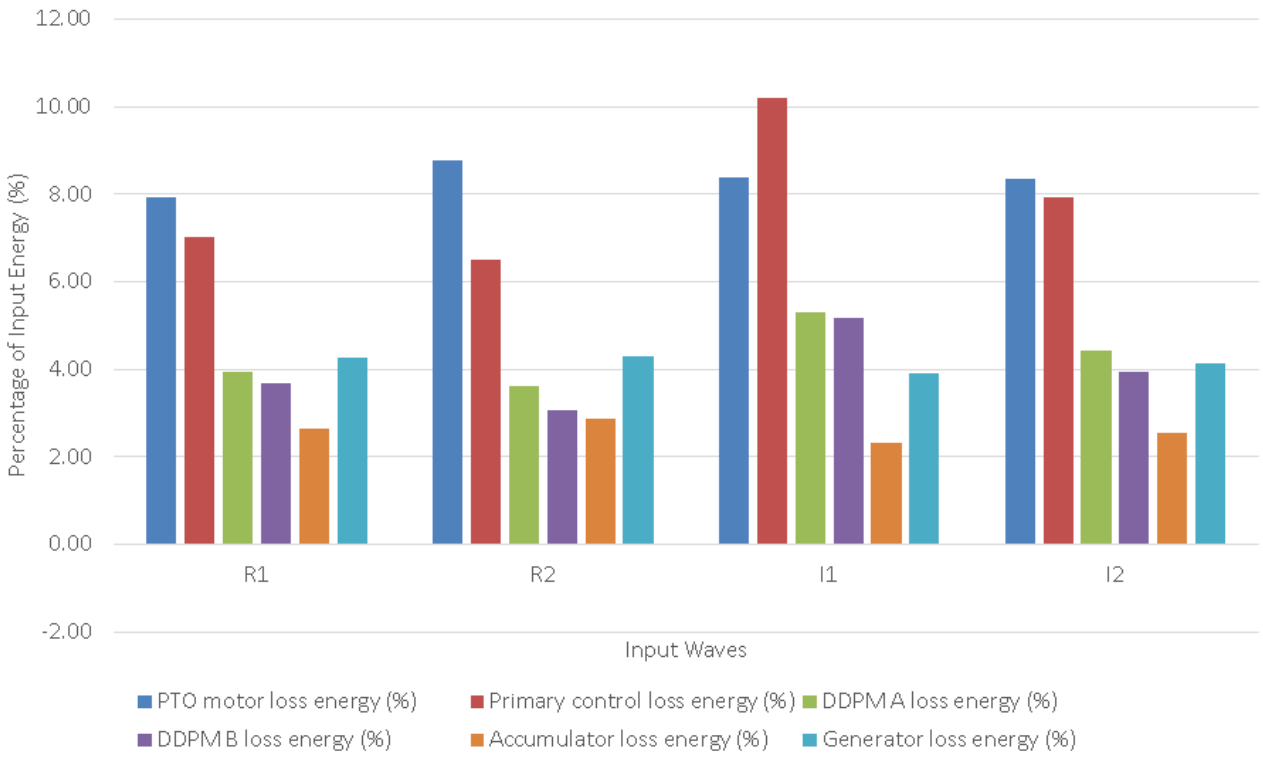

Fig. 7. Bar chart showing breakdown of energy lost for each wave input as a percentage of the total input shaft energy

to excessive additional losses, which suggests that the Quantor could operate in high energy saturation conditions in the sea. The PTO motor losses are higher in R2 than R1, due to flow losses and also due to partially bypassing of the DDPM while saturated and hence shedding a proportion of the bypassed energy as the pressure drops from the DDPM 'overdrive' pressure to the accumulator pressure. However the block losses and DDPM losses are slightly lower proportionally in this case. For the DDPMs this is because they are able to reach a more efficient operating point as they work with higher displacement.

I1 and I2 results show more variation, despite being closer in power density than R1 and R2. The efficiency of the Quantor in I2 is approximately 3.9% higher than I1. From Fig. 7 it is clear that the block internal losses are the major contributor to this difference, as they are proportionally much higher for I1. This is because a lower energy sea state involves more zero-crossings in the applied PTO torque, relative to the power extracted. In the case of the Quantor, this means that more valve transitions are involved as the direction of the applied PTO torque changes. In the quantised service a loss occurs every time a chamber is vented from high pressure to low pressure, which is every time the applied quantised moment is stepped down in magnitude. A similar loss occurs in the continuous service because during load reversals the continuously controlled chambers must vent any residual pressure between the minimum DDPM pressure and the tank pressure. During this simulation, the DDPM was assumed to be able to reliably control pressure to a minimum of 30bar, which may be pessimistic. Establishing this minimum continuously controlled pressure is an early target of upcoming lab tests. The DDPM losses reduce in I2 as they deliver higher flows on average.

An interesting comparison is between R1 and I2, which have similar wave power densities (45.9 and 46.9 kW/m of crest length respectively). The Quantor is only 1.9% less efficient in I2 than in R1, which demonstrates that it can cope well with the varying loads without prior knowledge of the incoming waves. Again, this difference is likely caused by the requirement for more zero-crossings and valve transitions in the irregular sea state. The primary and secondary conversion efficiencies of the Quantor in each set of input waves are shown in Fig. PTO 8. In all cases the secondary conversion efficiency is higher than the primary conversion efficiency, and varies very little between sea states, remaining around 91.1%. The primary conversion efficiencies for the regular waves are both over 79%, whereas they are 73.6% and 77.6% for I1 and I2 respectively. As discussed above, a different choice of PTO motor and lowering the minimum pressure on the stiff service may improve the primary conversion efficiency. The peak value of primary conversion efficiency of 79.9% is lower than that of 91.5% reported in [18] in irregular waves for a discrete displacement cylinder (DDC) system which was tested experimentally. The efficiency impact of rotary actuators compared to linear actuators may explain this difference.

[12] reports primary conversion efficiencies of over 80% which is higher than the results for the Quantor. The total wave-to-wire efficiency for Pelamis was over 70% [9], with a secondary conversion efficiency of approximately 90% for the P2 Pelamis. The primary conversion efficiency of the Quantor PTO cannot feasibly be as high as that of the Pelamis because the

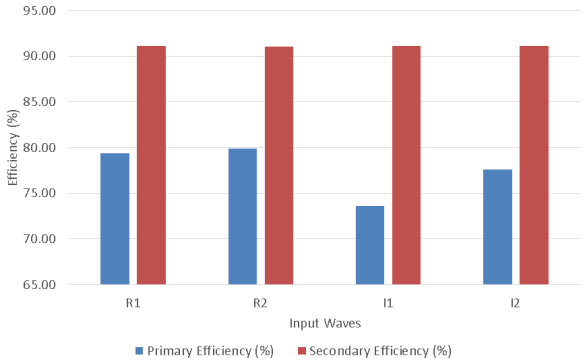

Fig. 8. Bar chart showing efficiency of primary and secondary conversion for each set of input waves.

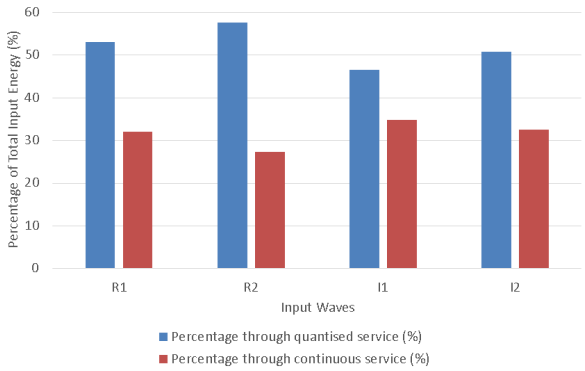

Fig. 9. Bar chart showing proportion of total input energy delivered through A (quantised) service and B (continuous) service.

continuously controlled service inherently has higher losses than the quantised service. However the continuous control should benefit the instantaneous power absorption and WEC control over the pure quantised control.

Fig. 9 shows the percentage of input energy which is delivered through the quantised (A) and continuous (B) services. The more energy that passes through the quantised service and the less through the continuous service, the higher the primary conversion efficiency. This is because DDPM B is generally at a less efficient operating point than DDPM A because it must go to lower displacements. The accumulator also acts as an energy store for the quantised service, but DDPM B must either instantaneously absorb the power available from the continuous service or lose it, as this service is very stiff. This result suggests that it is desirable for the quantised service to handle as much of the load as possible, with the continuous service only smoothing the response.

V. Model Evaluation

Valve opening times and pressurisation curves have already been validated with experimental data from a prototype manifold block. The PTO motor model is based on measured data from the manufacturers. The DDPM loss models are well-validated for pumping, and it is assumed that the motoring losses are the same since the loss mechanisms in this mode are the same. The auxiliary systems are difficult to model realistically, but every effort was made to accurately represent the physical dimensions and compliance of hydraulic connections. Fluid inertia was ignored as it would have been very computationally expensive to include, so this means that some transient effects may be missing. This was justified by carrying out a single model run in irregular seas with and without fluid inertia, which showed that the effect of fluid inertia on the average power transferred by key model components was very small. Whilst reasonable effort has been made to accurately model the hydraulic detail of the Quantor PTO, the true test of the model accuracy will be experimental validation on the test rig. The model may then be confidently extrapolated to larger rated powers and loads, and to different architectures. It is also anticipated that a validated simplified model of the PTO will allow rapid integration into third party WEC models for development of detailed WEC designs and control strategies.

VI. Conclusions and Further Work

A Simulink model of the Quantor PTO was constructed, which combines the quantising principle of the Pelamis PTO with AIP's DDPM machines. This combination should allow fully reactive WEC control, with the applied PTO torque smoothly matching the demand, while power is transmitted and converted with an efficiency similar to that of the quantised system. Reactive control and smooth PTO torque were shown in the detailed model, although obtaining smooth PTO torque required careful tuning of the control parameters. The detailed modelling of the hydraulics and mechanical systems allowed the various losses to be quantified at each stage of the power transmission. The Quantor PTO was simulated in a range of input waves, both regular and irregular, covering a wide range of power densities. The overall efficiency of the Quantor varies between 64.7% and 70.9%, which is very stable considering the variety in the input wave conditions. The Quantor performs well in irregular waves, with efficiency decreasing by only 2% between a regular and irregular wave set of similar power density. The largest sources of loss are the primary motors and the manifold blocks controlling flow to and from these motors, with the DDPM machines next. The easiest of these to improve is the primary motors where flow losses may be reduced with alternative choices. A system using linear actuators would have substantially lower primary losses, but would introduce end-stops and pressure shocks due to the larger chamber volume.

The Quantor performs more efficiently if a greater proportion of the energy is transferred through the quantised service and a smaller proportion is transferred through the continuous service. The Quantor system modelled here, and about to be physically tested, uses only 4 motors altogether, whereas an applied WEC system could use a larger number of motors with a commensurately larger proportion of energy being transmitted by the quantised service, which would offer increased efficiency. The primary conversion efficiency is slightly lower than that measured in previous studies of linear actuators, whilst the

secondary conversion efficiency seems comparable to that of Pelamis.

An experimental study of a Quantor prototype which will allow model refinement and validation is the most important piece of further work. A test rig is currently being commissioned on AIP's premises to enable this. A flywheel of significant inertia will be driven by an electric motor to emulate the hydrodynamic excitation and dynamic response of a WEC in regular and irregular waves. A Quantor PTO, matching that modelled, will be tested on this rig, extracting power from the emulated WEC and demonstrating combined quantised and continuous control. The data gathered will be invaluable for confirming the viability and efficiency of the Quantor PTO, and therefore its potential usefulness for WEC applications. There is also the possibility of simulating different fixed-displacement PTO motors, as well as simulating linear primary actuators. Different power ratings and architectures may also be extrapolated using the validated model elements. Control is another avenue for further work; once the model is fully validated new control features can be developed in the model environment.

ACKNOWLEDGEMENT

The authors gratefully acknowledge the support of Wave Energy Scotland and the EPSRC via the IDCORE programme.

REFERENCES

[1] K. Gunn and C. Stock-Williams, "Quantifying the global wave power resource," *Renewable Energy*, vol. 44, pp. 296–304, 2012. [Online]. Available: http://dx.doi.org/10.1016/j.renene.2012.01.101

[2] H. L. Bailey, "The effect of a nonlinear Power Take Off on a Wave Energy Converter," Ph.D. dissertation, University of Edinburgh, 2009. [Online]. Available: http://hdl.handle.net/1842/5741

[3] S. H. Salter, J. R. M. Taylor, and N. J. Caldwell, "Power conversion mechanisms for wave energy," *Proceedings of the I MECH E Part M*, vol. 216, no. 1, pp. 1–27, 2002. [Online]. Available: http://www.ingentaselect.com/rpsv/cgi-bin/cgi?ini=xref{\&}body=linker{\&}reqdoi=10.1243/147509002320382112

[4] Artemis Intelligent Power Ltd, "Hybrid Digital Displacement ® hydraulic PTO for wave energy WES Power Take Off Public Report," Tech. Rep., 2017. [Online]. Available: https://library.waveenergyscotland.co.uk/development-programmes/power-take-off/stage-2/pt21{_}art/

[5] R. Henderson, J. Macpherson, and J. Taylor, "Wave Energy Power Take-Off Competition Milestone 2 report " Hybrid Digital Displacement ® hydraulic PTO for wave energy "," Tech. Rep. January, 2016.

[6] J. Taylor and R. Henderson, "Wave Energy Power Take-Off Competition Milestone 1 report " Hybrid Digital Displacement ® hydraulic PTO for wave energy "," Tech. Rep. December, 2015.

[7] R. H. Hansen, *Aalborg Universitet Design and Control of the PowerTake-Off System for a Wave Energy Converter with Multiple Absorbers Hansen , Rico Hjerm Publication date :*, 2013.

[8] W. Sheng, R. Alcorn, and A. Lewis, "On improving wave energy conversion, part I: Optimal and control technologies," *Renewable Energy*, vol. 75, pp. 922–934, 2015. [Online]. Available: http://dx.doi.org/10.1016/j.renene.2014.09.048

[9] R. Yemm, D. Pizer, C. Retzler, and R. Henderson, "Pelamis: experience from concept to connection," *Philosophical Transactions of the Royal Society A: Mathematical, Physical and Engineering Sciences*, vol. 370, pp. 365–380, 2012.

[10] N. J. Caldwell, "Digital Displacement Hydrostatic Transmission Systems," Ph.D. dissertation, University of Edinburgh, 2007.

[11] W. H. S. Rampen, "The Digital Displacement Hydraulic Piston Pump," Ph.D. dissertation, University of Edinburgh, 1992.

[12] R. Henderson, "Design, simulation, and testing of a novel hydraulic power take-off system for the Pelamis wave energy converter," *Renewable Energy*, vol. 31, no. 2, pp. 271–283, 2006.

[13] E. No TitBrodtkorb, P.A., Johannesson, P., Lindgren, G., Rychlik, I., Rydén, J. and Sjö, "WAFO - a Matlab toolbox for analysis of random waves and loads," in *Proceedings of the 10th International Offshore and Polar Engineering Conference*, Seattle, 2000, pp. 343–350.

[14] J. Falnes, "A review of wave-energy extraction," *Marine Structures*, vol. 20, no. 4, pp. 185–201, 2007.

[15] A. F. Falcão and J. C. Henriques, "Effect of non-ideal power take-off efficiency on performance of single- and two-body reactively controlled wave energy converters," *Journal of Ocean Engineering and Marine Energy*, vol. 1, no. 3, pp. 273–286, 2015.

[16] Matlab, "2-way Directional Valve." [Online]. Available: https://uk.mathworks.com/help/releases/R2015b/physmod/hydro/ref/2waydirectionalvalve.html?searchHighlight=2waydirectionalvalve

[17] A. Pourmovahed, S. Baum, F. Fronczak, and N. Beachley, "Experimental evaluation of hydraulic accumulator efficiency with andwithout elastomeric foam," *Journal of Propulsion and Power*, vol. 4, no. 2, pp. 185–192, 1988.

[18] R. H. Hansen, T. O. Andersen, H. C. Pedersen, and A. H. Hansen, "Control of a 420kN Discrete Displacement Cylinder drive for the Wavestar energy converter," in *Proceedings of the ASME/BATH 2014 Symposium on Fluid Power & Motion Control*, Bath, UK, sep 2014, pp. 1–10. [Online]. Available: http://proceedings.asmedigitalcollection.asme.org/pdfaccess.ashx?url=/data/conferences/asmep/81754/